LOW-COST FIBER-OPTIC CHEMOCHROMIC HYDROGEN GAS DETECTOR

D. K. Benson[a], C. E. Tracy[a], G. A. Hishmeh[b], P. A. Ciszek[c], Se-Hee Lee[a], Roland Pitts[a] and D. P. Haberman[b]

[a]National Renewable Energy Laboratory, Golden, CO 80401
[b]DCH Technologies, Valencia, CA 91355
[c]Evergreen Solar, Waltham, MA 02451

ABSTRACT

Low-cost, hydrogen-gas-leak detectors are needed for many hydrogen applications, such as hydrogen-fueled vehicles where several detectors may be required in different locations on each vehicle. A fiber-optic hydrogen gas leak detector could be inherently safer than conventional detectors, because it would remove all detector electronics from the vicinity of potential leaks. It would also provide freedom from electromagnetic interference, a serious problem in fuel-cell-powered electric vehicles. This paper describes progress in the design of a fiber-optic, surface-plasmon-resonance hydrogen detector, and efforts to make it more sensitive, selective, and durable.

Chemochromic materials, such as tungsten oxide and certain Lanthanide hydrides, can reversibly react with hydrogen in air while exhibiting significant changes in their optical properties. Thin films of these materials applied to a sensor at the end of an optical fiber have been used to detect low concentrations of hydrogen gas in air. The coatings include a thin silver layer in which the surface plasmon is generated, a thin film of the chemochromic material, and a catalytic layer of palladium that facilitates the reaction with hydrogen. The film thickness is chosen to produce a guided-surface plasmon wave along the interface between the silver and the chemochromic material. A dichroic beam-splitter separates the reflected spectrum into a portion near the resonance and a portion away from the resonance, and directs these two portions to two separate photodiodes. The electronic ratio of these two signals cancels most of the fiber transmission noise and provides a stable hydrogen signal.

Keywords: fiber-optic, hydrogen, sensor, thin-film, surface-plasmon resonance, chemochromic, tungsten oxide, yttrium hydride

1. INTRODUCTION

The ability to detect hydrogen gas leaks economically and with inherent safety is an important technology that could facilitate commercial acceptance of hydrogen fuel in various applications. In particular, hydrogen-fueled passenger vehicles will require hydrogen leak detectors to signal the activation of safety devices such as shutoff valves, ventilating fans, and alarms. Such detectors may be required in several locations within a vehicle—wherever a leak could pose a safety hazard. It is therefore important that the detectors be very economical. This paper reports progress on the development of low-cost, fiber-optic hydrogen detectors intended to meet the needs of a hydrogen-fueled passenger vehicle.

In our design, a thin-film coating at the end of a polymer optical fiber senses the presence of hydrogen in air. When the coating reacts reversibly with the hydrogen, its optical properties are changed. Light from a central electro-optic control unit is projected down the optical fiber where it is reflected from the sensor coating back to central optical detectors. A change in the reflected intensity indicates the presence of hydrogen. The fiber-optic detector offers inherent safety by removing all electrical power from the leak sites and reduces signal-processing problems by minimizing electromagnetic interference. Critical detector performance requirements include high selectivity, response speed, and durability as well as potential for low-cost production.

Ito[1] originally proposed using the palladium-catalyzed reaction of amorphous tungsten oxide with hydrogen in a fiber-optic hydrogen detector. The reaction causes partial reduction of the tungsten oxide and introduces a strong optical-absorption band near 800 nm. The increase in absorption reduces the intensity of the light beam reflected by the coated optical fiber. We found this sensor design to be adequately sensitive, but too slow for the intended use.

A different sensor design using a surface-plasmon resonance (SPR) configuration[2] was also evaluated. The SPR shifts in response to very subtle changes in the refractive index of the coating. This shift can be monitored to provide a faster response.

2. EXPERIMENTAL METHODS

2.1 Coatings

Thin-film sensor coatings were deposited by thermal evaporation. Tungsten oxide powder (99.9%) was evaporated from a resistively heated tungsten effusion source. Palladium, silver, yttrium and gold metals were evaporated from tungsten boats. All depositions were monitored with a quartz crystal deposition rate monitor. Film thickness was measured with a stylus gauge.

2.2 Chemochromic Response Measurements

Most of the thin films' sensors were deposited on 20-mm, right angle prisms for easier characterization. The test apparatus was designed to seal the coated surface from the surrounding air and expose it to a flow of a predetermined gas mixture (Fig. 1). Small percentages of hydrogen in air were simulated by mixing measured flows of oxygen and nitrogen with prepared sources of 10% and 1% hydrogen in nitrogen. A synthetic air source was used for flushing the sample between test runs. A fiber-optic white light source illuminated the coating through one leg of the prism, and a fiber-optic detector gathered reflected light through the other leg of the prism and directed it to a diode array spectrophotometer (Ocean Optics model S2000). The locations of the ends of the fibers (functioning as entrance and exit apertures) were fixed so that only light internally reflected by the sensor coating at a 45° angle would reach the spectrometer. Fast toggle valves on the gas-mixing manifold and timed acquisition of spectra made it possible to measure the optical reflectance spectra as a function of time and to calculate the response time constant of the sensor.

2.3 Optical Modeling

The spectral transmittance, reflectance, and other optical characteristics of the sensor films were modeled using commercial software.[3] This software also solves the equations for the SPR condition and accurately predicts the reflectance spectra. Most of the optical constants for modeling the various materials used in the sensors were obtained from the American Optical Society.[4] The optical properties of tungsten-oxide thin films with various amounts of hydrogen "inserted" (commonly referred to as H_xWO_3) were approximated using measured optical data for tungsten-oxide films with lithium electrochemically "inserted" (Li_xWO_3).[5]

3. RESULTS

3.1 Evaluation of Sensor Coatings

Simple reflective sensors, without surface plasmon resonance, were used for preliminary tests. The end of a polymer optical fiber was coated with 500 nm WO_3 and a superficial layer of 10 nm palladium. Figure 2 shows a calibration curve obtained from such a sensor in air with various concentrations of hydrogen. The reflected signal at 850 nm is attenuated by the optical absorption in the WO_3 in proportion to the reaction with hydrogen, which in turn is proportional to the hydrogen concentration. The sensitivity is adequate for detection of the hydrogen well below the lower explosion limit of 4% in air.

Figure 3 shows theoretical reflectance spectra for a tungsten-oxide sensor film in an SPR configuration. The sensor film consists of a stack of two layers: a 40 nm thick layer of gold and a 600 nm thick layer of WO_3. The shift in this spectrum from curve a to b is the predicted result of the "insertion" of hydrogen to a level of $H_{0.068}$ WO_3. In this model, as in the sensor test configuration, the incident light strikes the film from inside the glass prism at 45°, an angle that is greater than the angle for total internal reflection. Without the coating, all of the light would be reflected. However, at the resonance wavelength, the electric field of the incident light interacts resonantly with the free electrons in the gold to set up an electrical charge oscillation at the glass/gold interface. This is a so-called SPR. The wavelength at which the resonance occurs is strictly a function of the optical dielectric constants of the glass and

gold. The light energy at this wavelength is dissipated by electrical losses in the gold and by re-radiation of the light by the electrons in all directions.

This SPR condition can be reinforced by the right choice of tungsten oxide thickness such that a constructive interference occurs at the resonance wavelength in the oxide layer. Under these conditions, the gold/WO_3 stack acts like a pair of coupled resonators, and both the resonance wavelength and the resonance amplitude depend sensitively upon the optical dielectric constants of the glass, the gold, and the WO_3. When the hydrogen reacts with the tungsten oxide, the oxide refractive index decreases and the resonance shifts as indicated in Fig. 3.

The reaction of hydrogen and tungsten oxide is too slow without a catalyst. A thin layer of a catalyst such as palladium must be added. The palladium tends to absorb the resonance wavelength light and dampen the resonance. Figure 4 shows the theoretical reflectance spectrum from a sensor coating consisting of 40 nm gold/600 nm WO_3/3 nm Pd. Note that the optical model assumes uniform optical properties for the various layers, whereas the 3 nm Pd layer was discontinuous. For comparison, we show a measured reflectance spectrum from a sensor coating of this same configuration. The spectral characteristics of the light source and the light detector have not been removed, so the measured spectrum contains more structure than the theoretical one, but the SPR can be clearly seen. This resonance wavelength was very stable, with no significant shift detected over the temperature range tested from 24° to 69°C.

Figure 5 shows a set of spectra from a time series taken during exposure to 5% hydrogen in air at room temperature. The inset shows the change in reflected light intensity at the resonant wavelength over time. The change in signal amplitude is approximately exponential with a time constant of about 20 s. Similar measurements were made over a range of hydrogen concentrations, and the time constant was found to decrease as the concentration increased. Over a range of hydrogen concentrations up to 5%, the relationship between time constant, τ and partial pressure, P_{H2} appeared to be:

$$\tau \propto P_{H2}^{-2}$$

Unfortunately, the tungsten oxide readily exchanges water vapor with the atmosphere. Water adsorbed onto the nano-porous structure of the WO_3 increases its refractive index. Conversely, exposure of the sensor to dry air causes rapid loss of adsorbed water from the film and a shift in the SPR that mimics exposure to hydrogen.

A protective layer of poly-tetrafluoroethylene was applied over the palladium by thermal evaporation. This retarded the exchange of water vapor without significantly affecting the SPR and the sensitivity to hydrogen. However, the sensor SPR was still susceptible to severe drift under conditions of changing humidity.

Increasing the thickness of the palladium film to serve both catalytic and protective functions was also unsuccessful. Because the palladium absorbs resonance light and tends to broaden the SPR, implementing this design option is difficult. However, if the film thicknesses are chosen correctly, a constructive interference resonance condition that coincides with the SPR can be made to occur between the gold and palladium layers. Figure 6 shows the theoretical and measured reflectance spectra from such a coating in the SPR configuration (45° incidence angle).

Measurements with this sensor film design confirmed that it was only very weakly sensitive to prolonged exposure to humidity while remaining sensitive to hydrogen. Figure 7 shows the response of the sensor during exposure to 0.9% hydrogen in air. The response time constant is a few seconds. Over time, however, this response time increased dramatically. Figure 8 shows the measured response time for such a sensor over a period of 3 days. The time constant is seen to increase from a few seconds to more than 200 s, approximately increasing in proportion to the square root of time the sensor was exposed to the test gases.

Similar tests with a different chemochromic sensor (a YH_2/Pd coating) showed similar degradation – strongly suggesting that the degradation is related to “poisoning” of the palladium. We tested this possibility by overcoating the palladium with a superficial layer of tungsten oxide. The tungsten oxide is an oxidative catalyst and that serves to oxidize and remove poisons such as CO, H_2S, methane and other trace contaminants in the hydrogen test gases. Figure 8 shows the preliminary, but encouraging results for a WO_3/Pd/WO_3 sensor coating in comparison with the

original WO_3/Pd sensor coating. No degradation in response speed was observed over a period of several days when this sensor was tested in exactly the same way as the original sensor, which degraded severely within two days.

Recent research[6,7] has shown that the Lanthanide and related rare earth hydrides undergo reversible transitions between di-hydride and tri-hydride when exposed to hydrogen in air. Thin films of these materials exhibit dramatic changes in optical transmittance that may make them suitable for hydrogen sensing in our fiber-optic configuration.

Figure 9 shows a preliminary measurement of the reflectance from a yttrium-hydride film during repeated exposure to 0.45% hydrogen in air. The sensor film was not optimized, and yet its response time constant was fairly short—about 5.8 s. Experiments were conducted on similar samples over a range of temperatures in order to judge the suitability of this sensor for automotive applications where a wide operational temperature range will be required.

Figure 10 shows a typical hydrogen response in more detail. The decay in reflected light intensity corresponds to the decrease in reflectance of the YH_x as it reacts with the hydrogen and tends toward YH_3. The form of the response curve is a double exponential decay with a faster and a slower component. It is interesting that the faster response occurs after the slower response. We speculate that the faster response occurs after the composition of the YH_x film has changed to approximately YH_2 and is proceeding toward YH_3. A similar two time-constant, double exponential form also fits the sensor recovery in oxygen.

Figure 11 shows Arrhenius plots of the hydrogen response and recovery time constants for a YH_2/Pd sensor over a range of temperatures. The slope of these plots is consistent with an activation energy of about 0.4 eV/molecule for both the hydrogen response and the recovery in oxygen. This is a significantly lower activation energy than the 0.77 eV we had previously measured for the WO_3 sensor and suggests that the YH_2 sensor would be easier to use over a wide temperature range.

3.2 Prototype Hydrogen Gas Leak Detector

A self-contained, hand-held portable fiber-optic hydrogen detector was designed and built. The light source is a high-brightness, broad-spectrum "white" (phosphor-enhanced) LED. The light from the LED is projected into the proximal end of a 1-mm-diameter polymer optical fiber and transmitted through a 1 x 2 coupler to an exit port on the instrument. The optical-fiber sensor is plugged into that port with a standard fiber-optic ST connector. Light reflected from the sensor coating on the distal end of the fiber is returned to the instrument, and half of its power is directed through one of the coupler legs to a dichroic mirror. The dichroic mirror splits the return light beam into long- and short-wavelength portions that fall separately on two different photo-diode amplifiers. The voltage signals from the two photo-diodes are divided one by the other in an analog divide circuit. Figure 12 shows a schematic illustration of the detector's design features.

When used with a WO_3/Pd sensor coating on the end of an optical fiber in a purely reflective mode (no SPR), the light reflected from the sensor is split into a short-wavelength component ($\lambda < 500$ nm) and a long-wavelength component ($\lambda > 500$ nm). When the tungsten-oxide film reacts with hydrogen it develops an absorption band in the near-infrared portion of the spectrum, but remains unaffected in the blue end of the spectrum. Thus, the long-wavelength portion of the spectrum carries a hydrogen signal, whereas the short-wavelength portion does not and can be considered as a "reference" signal.

Because both components of the spectrum follow the same path through the optical fiber, they are both affected similarly by changes in the transmittance through the fiber. Taking the ratio of the "signal" to the "reference" provides a means of canceling some of the changes in fiber transmittance, whatever its cause, and thereby reduces the noise level. Transmittance can be affected by bending in the fiber, by temperature gradients in the fiber, and by changes in the light transmittance at the connections.

Figure 13 shows some measurements of the effect of fiber bending. The conditions at the instrument and at the sensor were kept constant, and the signals returning to the instrument were recorded as the meter-long polymer optical fiber was intentionally bent through an increasingly sharp radius. The bend in the fiber caused reversible optical losses and attenuated the intensity of the reflected beam. In the figure, the percentage change in the signal voltage from each photo-diode caused by fiber bending is shown separately along with the analog ratio of the two voltages. It is clear that the use of a reference signal greatly decreases the effect of fiber bending.

To produce a sharp SPR in the sensor film, the light beam must strike the film at a single angle. In our design, where we want the reflected light to be returned along the same fiber path, the preferred angle is 45°, and the best shape for the sensor "head" is a 90° prism acting as a retro-reflector.

It is necessary to collimate the diverging exit beam from the optical fiber before directing it through the prism to the sensor coating. For this purpose, an optode was designed that contains an aspheric plano-convex lens and a 90° prism. The sensor coating is applied to one face of the prism. The optode is designed to be a small, single component that could be mass-produced by die-injection polymer molding. A commercial, optical ray-tracing code was used to generate the design for the optode.[8]

The optode consists of a plano-convex lens integrally combined with a 90° prism. A simple spherical convex lens surface is not sufficient to collimate the emerging broad-spectrum beam and focus the reflected light back onto the 1-mm-diameter fiber tip. Therefore, a conic surface was used in the optimization of the optode (2.85-mm curvature radius, 2.055 conicity, 5.1-mm FL). Figure 14 illustrates the optimized optode design, assuming that it will be made from polymethylmethacrylate (PMMA) and will be coupled to a polymer optical fiber having a numerical aperture of 0.5.

Because of the expense of fabricating a single component of this design, we also designed an non-optimum optode that could be easily fabricated by cementing a commercially available stock BK7 glass plano-convex lens (10-mm diameter, 15-mm FL, 7.73-mm curvature radius) to a glass 90° prism. Several glass optodes of this design were fabricated and coated with a sensor film (15 nm Ag/440 nm WO_3 /35 nm Pd). A holder was made to attach the optode to the optical fiber. Figure 15 shows the spectra of the reflected light: a, theoretical (assuming a perfectly collimated beam at an incidence angle of 45°); and b, the measured spectrum. There is a close correlation between the theoretical and the measured spectra, even though the spherical plano-convex lens is less than optimum.

4. DISCUSSION

4.1 Sensor Films

The thin-film, fiber-optic reflective sensor based on palladium-catalyzed WO_3 first suggested by Ito[1] appears to work well for detecting hydrogen. However, its response is too slow for some safety applications. We showed that the sensitivity and the response speed of this sensor could be increased by use of a film configuration that produces a SPR. The long-term stability and durability of this sensor coating remains to be demonstrated. The use of a superficial coating of tungsten oxide over the hydrogen dissociation palladium catalyst layer shows some promise for reducing contamination of the palladium by common poisons whose oxidation can be catalyzed by the WO_3.

Yttrium di-hydride and related sensor materials may have some advantages over the tungsten oxide sensor. The di-hydrides appear to be less susceptible to changes caused by adsorption/desorption of water vapor and the YH_2 reaction with hydrogen has a significantly lower thermal activation energy. These differences may make the YH_2 sensor coating design better suited for the automotive application.

4.2 Detector

The use of a fiber-optic, hydrogen-gas-leak detector has advantages of inherent safety (no electrical power in the vicinity of the sensor), reduced electromagnetic interference, lightness of weight, and (potentially) low cost. Most, if not all, of the needed electro-optic components could be integrated into a single application-specific integrated circuit (ASIC) for economical mass production. An analysis of the probable manufacturing costs has shown that it should be possible to mass-produce similar detectors for about $5 each (not including the cost of the polymer optical fiber). [13]

5. CONCLUSIONS

The development of a fiber-optic, chemochromic, hydrogen gas detector has been partially successful, but more work is required to develop a durable sensor coating. The chemochromic reaction between tungsten oxide and hydrogen in air may be too slow to be used in some safety devices without some kind of enhancement. The sensitivity and speed

of hydrogen detection can be enhanced by using the sensor film in a surface plasmon resonance (SPR) configuration. However, in such a configuration, any change in optical properties of the sensor coating will cause a shift in resonance wavelength and the detector becomes susceptible to unintended side reactions, both chemical and physical. For example, the rapid desorption of adsorbed water vapor from the tungsten oxide can cause a false indication of hydrogen whenever the sensor is exposed to a dry gas.

Preliminary experiments with yttrium di-hydride chemochromic sensor coatings showed promising speed and sensitivity in a simple sensor configuration. Optimization of the YH_2 sensor design, including the use of SPR, may provide the needed combination of sensitivity and speed with less susceptibility to interferences.

6. ACKNOWLEDGMENTS

The authors would like to acknowledge valuable assistance provided by M. Rubin and K. von Rottkay at the Lawrence Berkeley National Laboratory. The U. S. Department of Energy's Hydrogen R&D Program supported this research under Contract No. DE-AC-36-83CH10093.

7. REFERENCES

1. K. Ito and T. Kubo, "Gas Detection by Hydrochromism," In *Proceedings of the 4th Sensor Symposium*, pp. 153–156. 1984.
2. H. Raether, *Surface Plasmons*, p 21, Berlin: SpringerVerlag. 1988.
3. A. Macleod, The Essential Macleod Thin-film Design Software User Manual, Tucson, AS: The Thin Film Center. 1995.
4. E. D. Palik, ed., *Handbook of Optical Constants Diskette*, Optical Society of America, Washington, DC. 1995.
5. K. Von Rottkay, M. Rubin, and N. Ozer, "Optical Indices of Tin-Doped Indium Oxide and Tungsten Oxide *Proceedings Material Research Society Symposium*, Vol. 403, pp. 551–556, 1996.
6. R. Griessen et al., "Yttrium and Lanthanum Hydride Films with Switchable Optical Properties," *J. Alloys and Compounds*, 253–254:44–50. 1997.
7. J.N. Huiberts et al., "Synthesis of Yttriumtrihydride Films for Ex-situ Measurements," *J. Alloys and Compounds*, 239:158–171. 1996.
8. Anon., Zemax Optical Design Program User's Guide, Version 7.0, Focus Software, Tucson, AZ, 1998.
9. C.G. Granqvist, Handbook of Inorganic Electrochromic Materials, New York: Elsevier. 1995
10. J-G Zhang, D.K. Benson, C.E. Tracy, S.K. Deb, A.W. Czanderna, and C. Bechinger, "Electrochromic Mechanism in a-WO_3 Films," *J. Electrochem. Soc*., 96-24:251–259. 1996.
11. Wagner, W., F. Rauch, C. Ottermann, and K. Bange Wagner. 1990. *Nuclear Instr. Methods. Phys. Res. B*., 50:27.
12. C. Bechinger, G. Oefinger, S. Herminghaus, and P. Leidered. "On the Fundamental Role of Oxygen for the Photochromic Effect in WO_3." *J. Appl. Phys.*, 74:4527–4533. 1993.
13. P.L. Spath and D.K. Benson. "An Economical Hydrogen Detector for Passenger Vehicles," In *Proceedings of the Second Hydrogen Power, Theoretical and Engineering Solutions, International Symposium (HYPOTHESIS)*, Aug. 18–22, 1997, Grinstad, Norway. 1997.

8. FIGURES

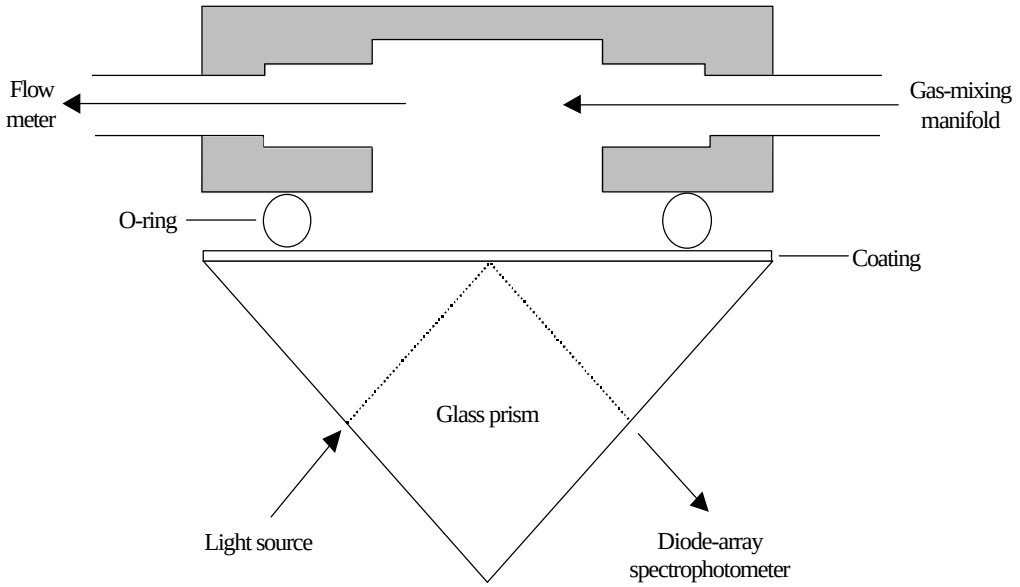

Figure 1. Schematic cross-section through the SPR sensor sample holder.

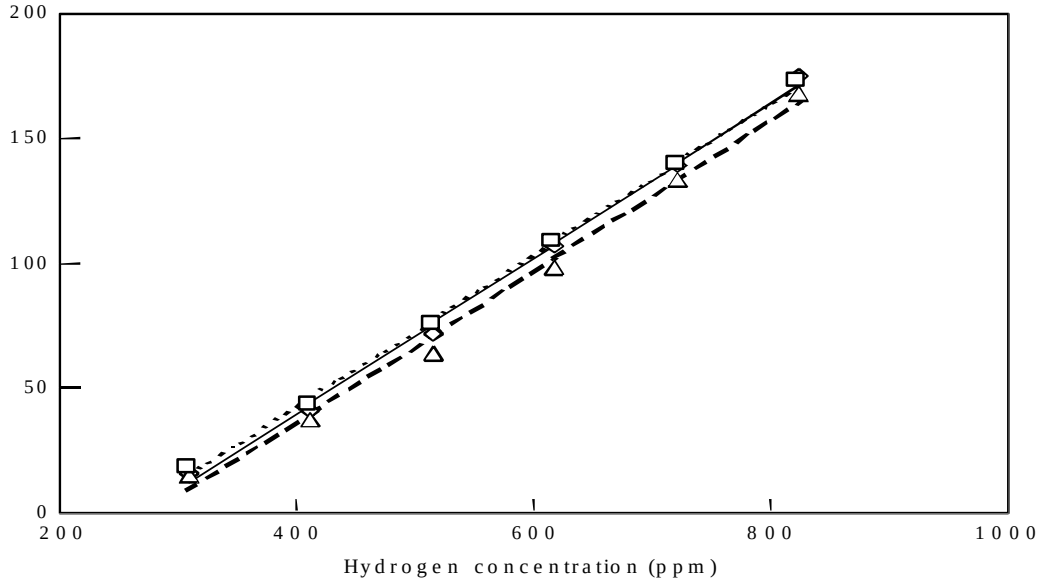

Figure 2. Calibration curves for a simple reflective WO_3/Pd-coated F-O sensor.

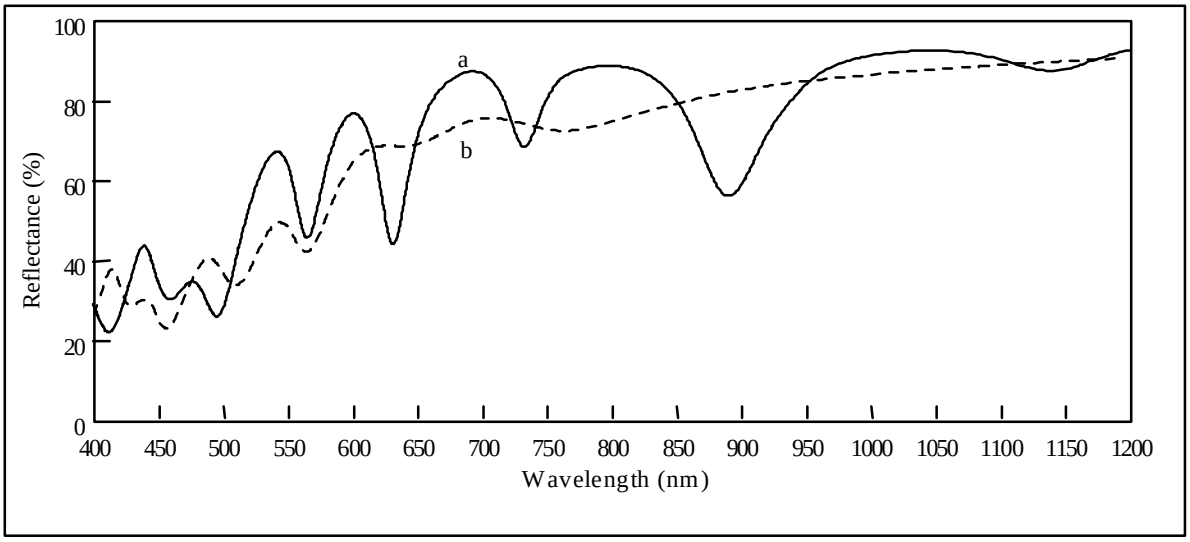

Figure 3. Theoretical reflectance spectra showing the SPR absorption at 640 nm: a, before exposure to hydrogen; b, after reaction with hydrogen to form (nominally) $H_{0.068}WO_3$. Coating consists of 40 nm Au/600 nm WO_3 and is illuminated at 45°.

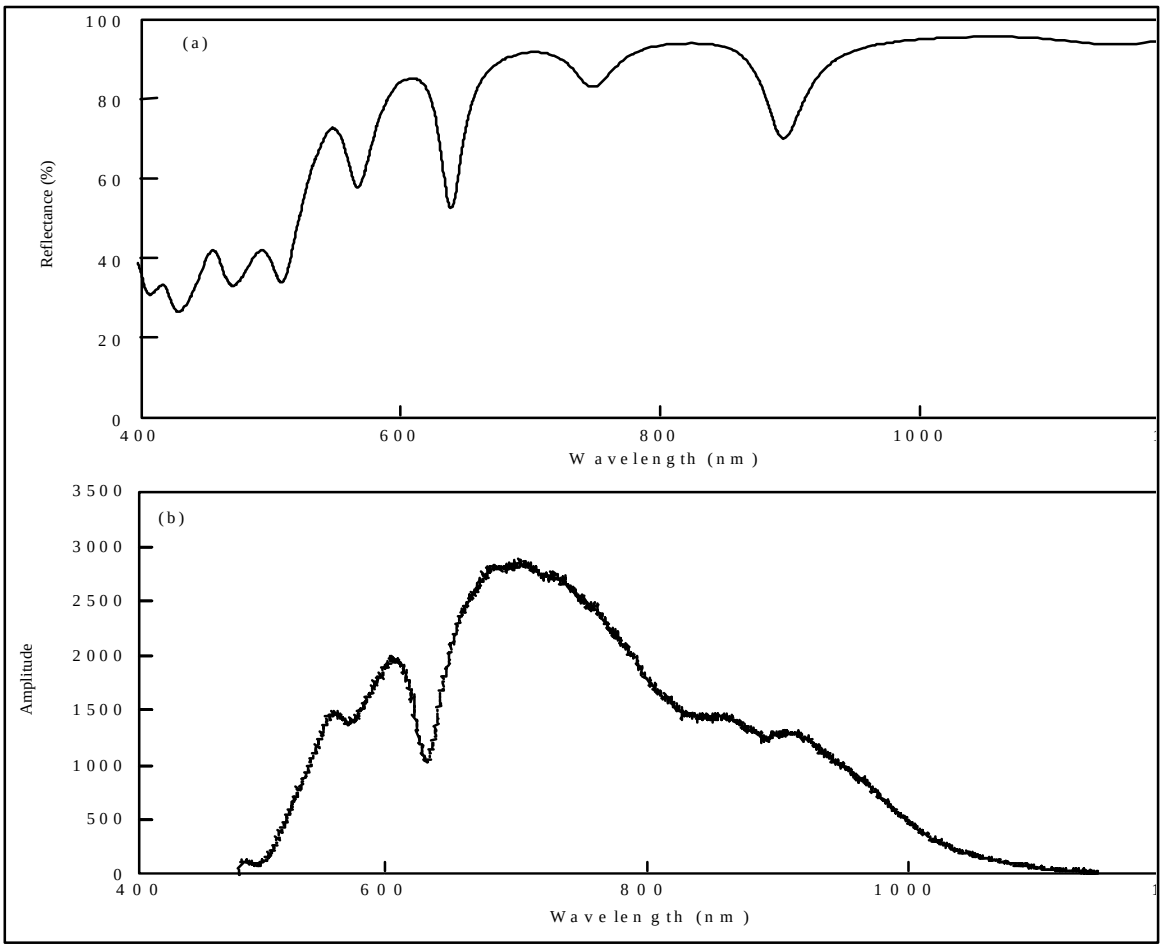

Figure 4. Reflectance SPR spectra from a coating of 40 nm Au/600 nm WO_3/3 nm Pd: a, theoretical; b, measured.

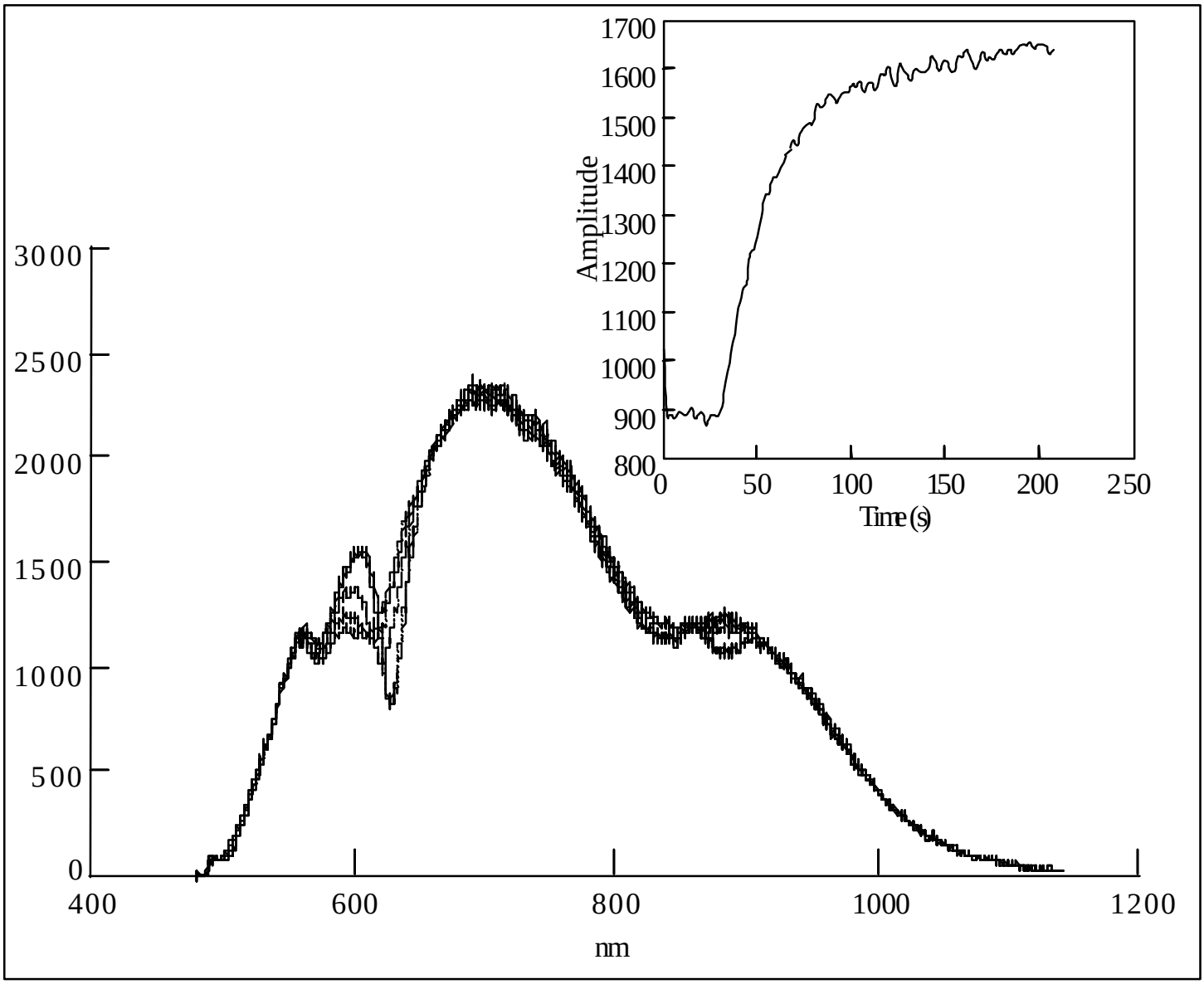

Figure 5. Selected reflectance spectra from a time series during exposure to 5% H_2 in air.

The inset shows reflected intensity at 627 nm versus time. The coating is 40 nm Au/600 nm WO_3/3 nm Pd.

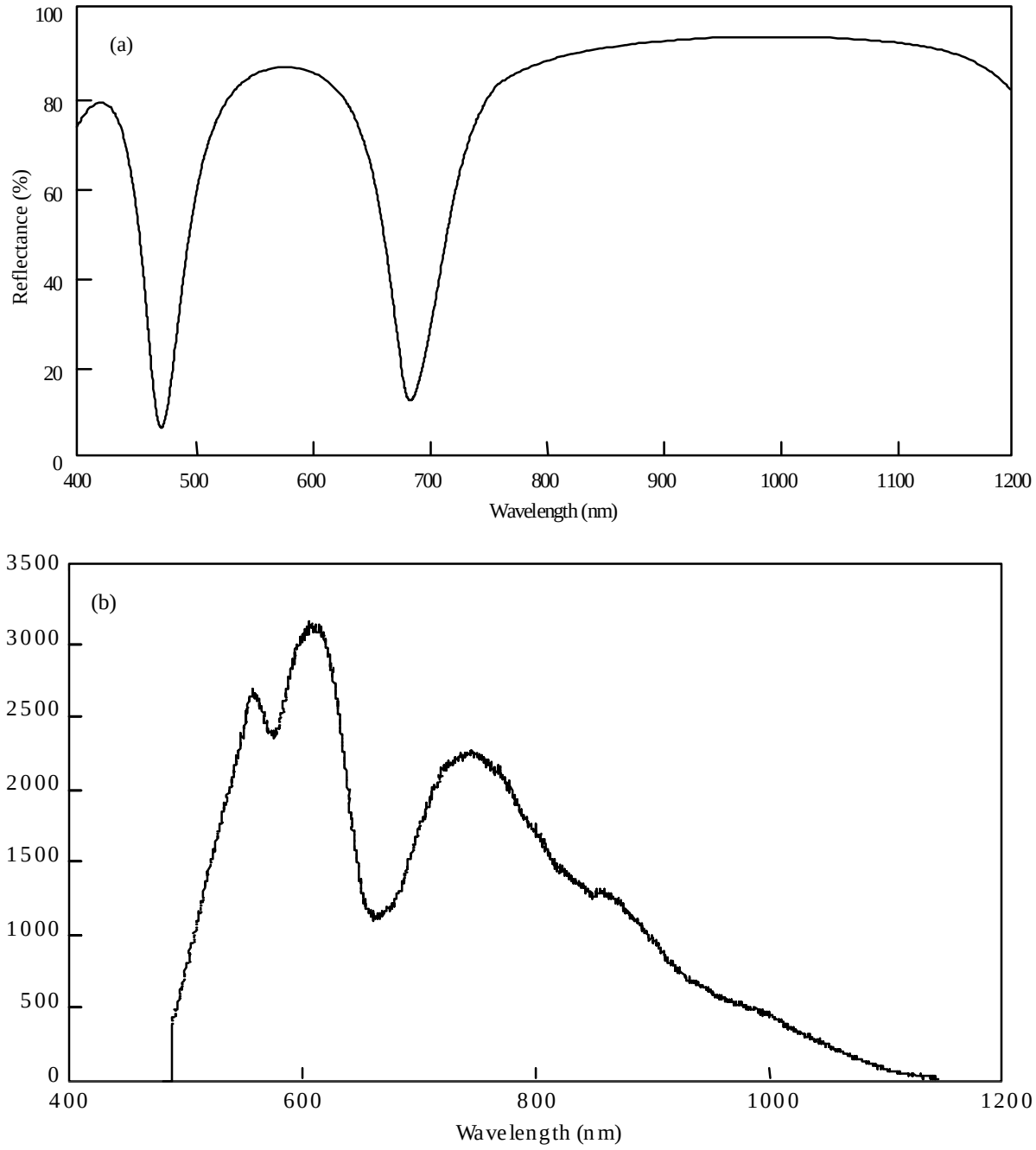

Figure 6. Reflectance SPR spectra from a coating with a thicker palladium layer: 17 nm Ag/330 nm WO_3/100 nm Pd: a, theoretical; b, measured.

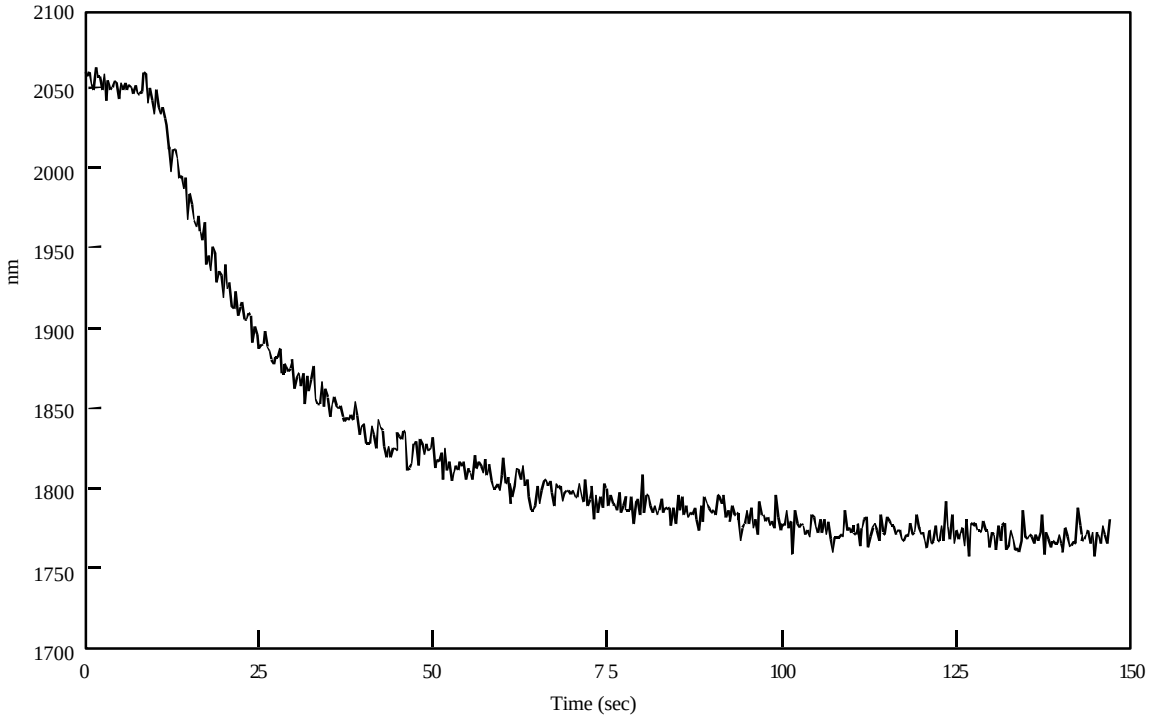

Figure 7. Initial response of sensor coating (17 nm Ag/330 nm WO_3/100 nm Pd) to 0.9% H_2 in air.

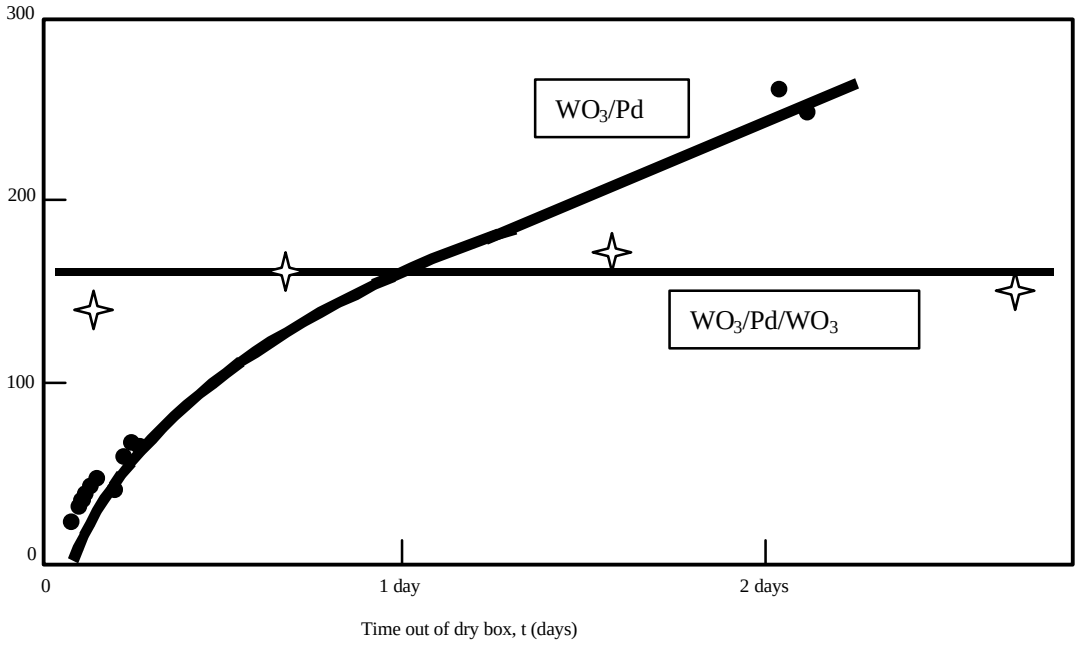

Figure 8. Sensor response time constant for film (17 nm Ag/330 nm WO_3/100 nm Pd) over a period of 2 days. The sample was exposed to 5% H_2 in air for periods of about 2 minutes, then to dry air. The response time constant was measured at 800 nm (about 200 nm away from the resonance). The fitted curve varies as the square root of time.

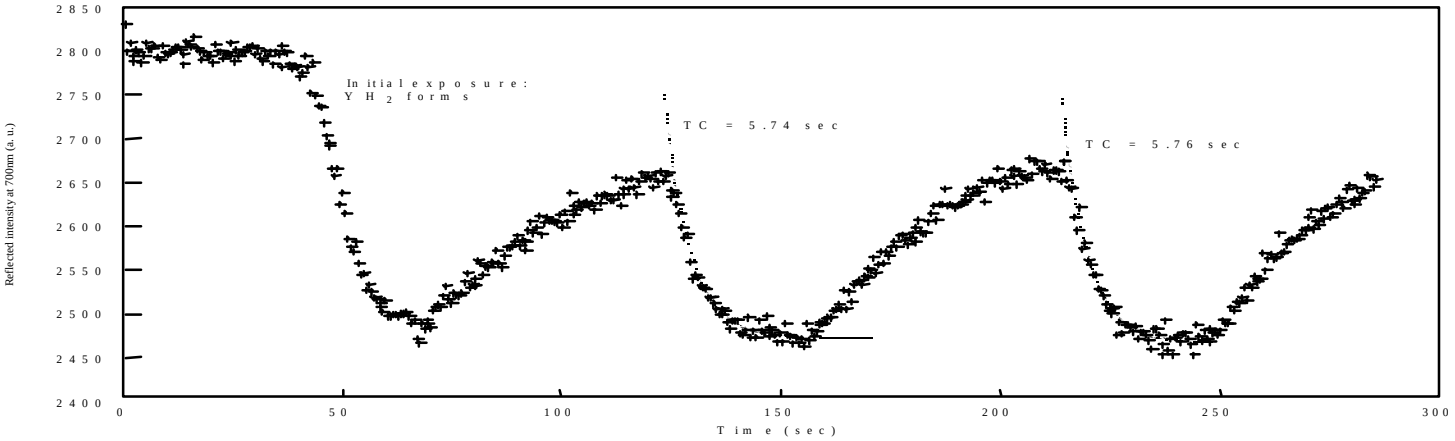

Figure 9. Initial response measurements for a yttrium-hydride film (17 nm Ag/100 nm Y/20 nm Pd) to 0.45% H_2 in air. The first reduction in the signal corresponds to conversion of Y metal to YH_2, and subsequent cycles to increases in hydrogen content toward the tri-hydride, YH_3. The response was measured in reflection (no SPR) at 700 nm. The time constant of the hydrogen response is about 5.7 seconds.

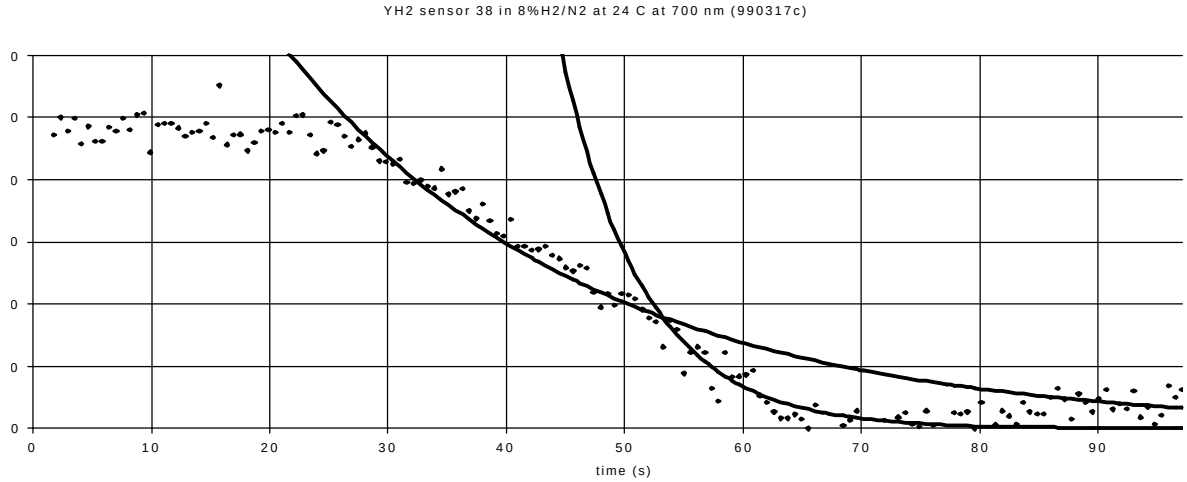

Figure 10. Response of a YH2 sensor to 8% H2/N2 mixture. Note the initially slower response followed by a faster response.

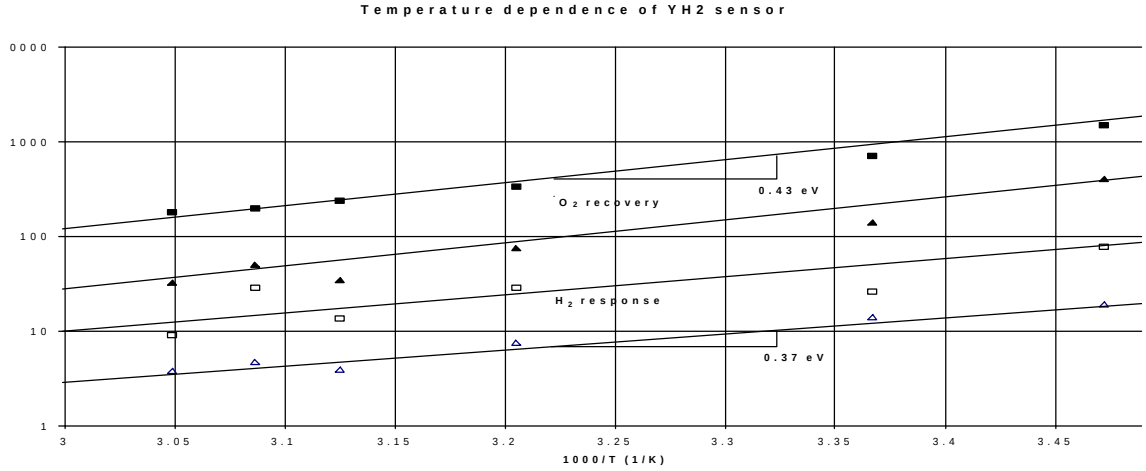

.Figure 11. Arrhenius plot of YH2 sensor time constant showing exponential temperature dependence with an activation energy of about 0.4 eV for the hydrogen response and the recovery in oxygen

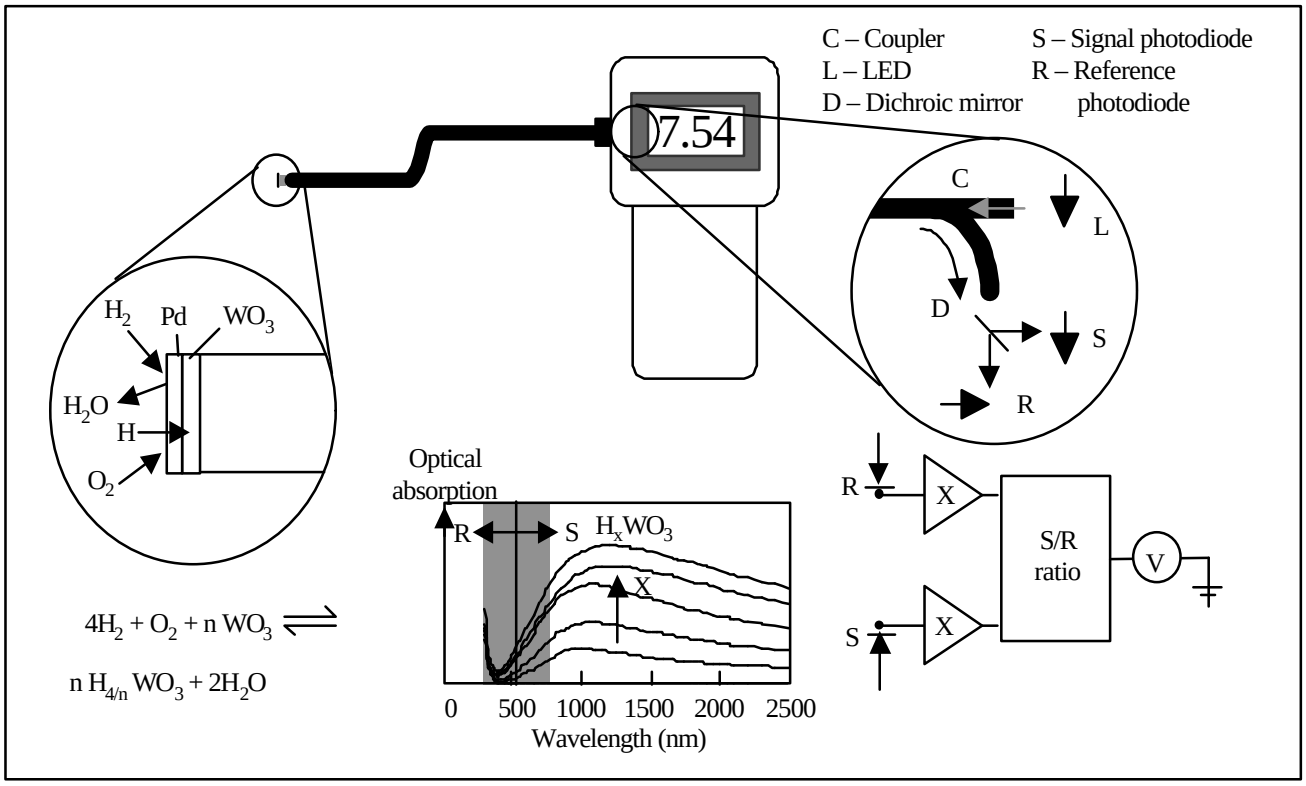

Figure 12. Schematic diagram of the prototype portable fiber-optic, hydrogen-gas-leak detector showing selected design features.

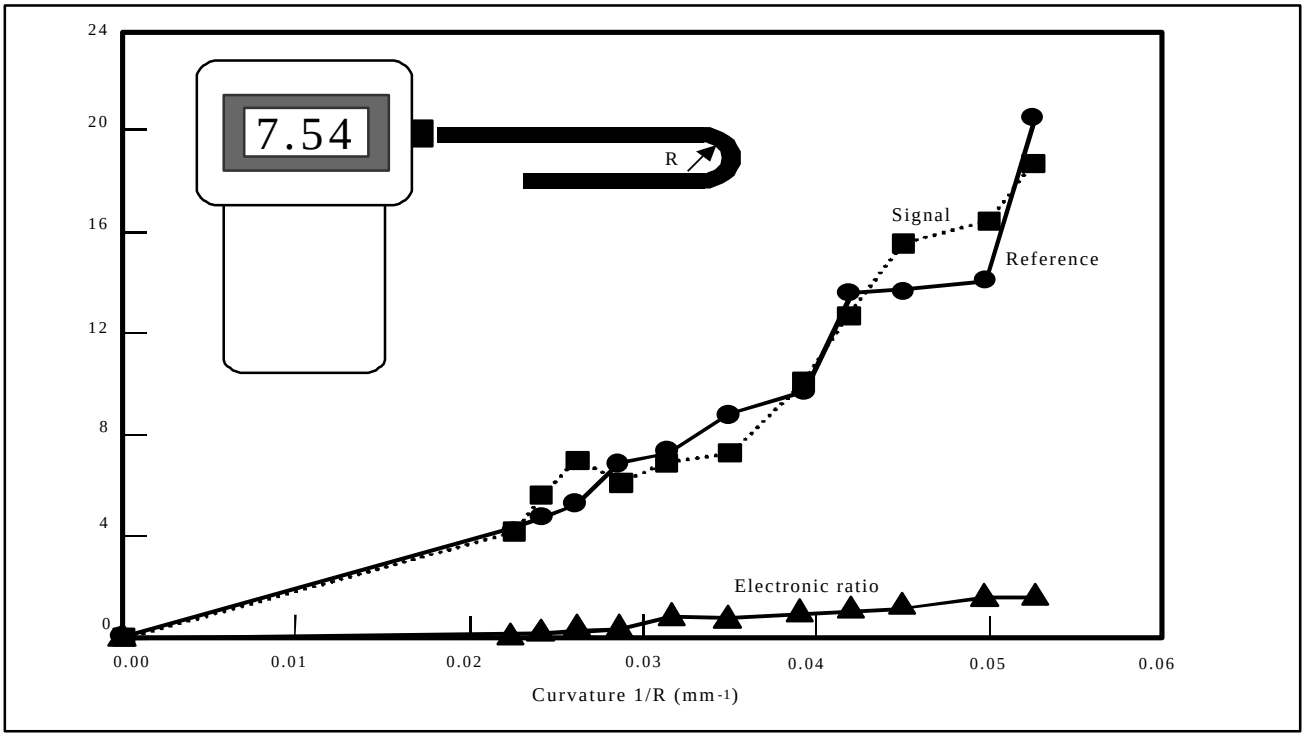

Figure 13. Detector signal attenuation due to controlled bending of the optical fiber. Note that the attenuation is nearly the same for the hydrogen signal (long wavelength) and the hydrogen-insensitive reference signal (short wavelength). Consequently, the analog ratio of the two signals is only weakly attenuated by fiber bending.

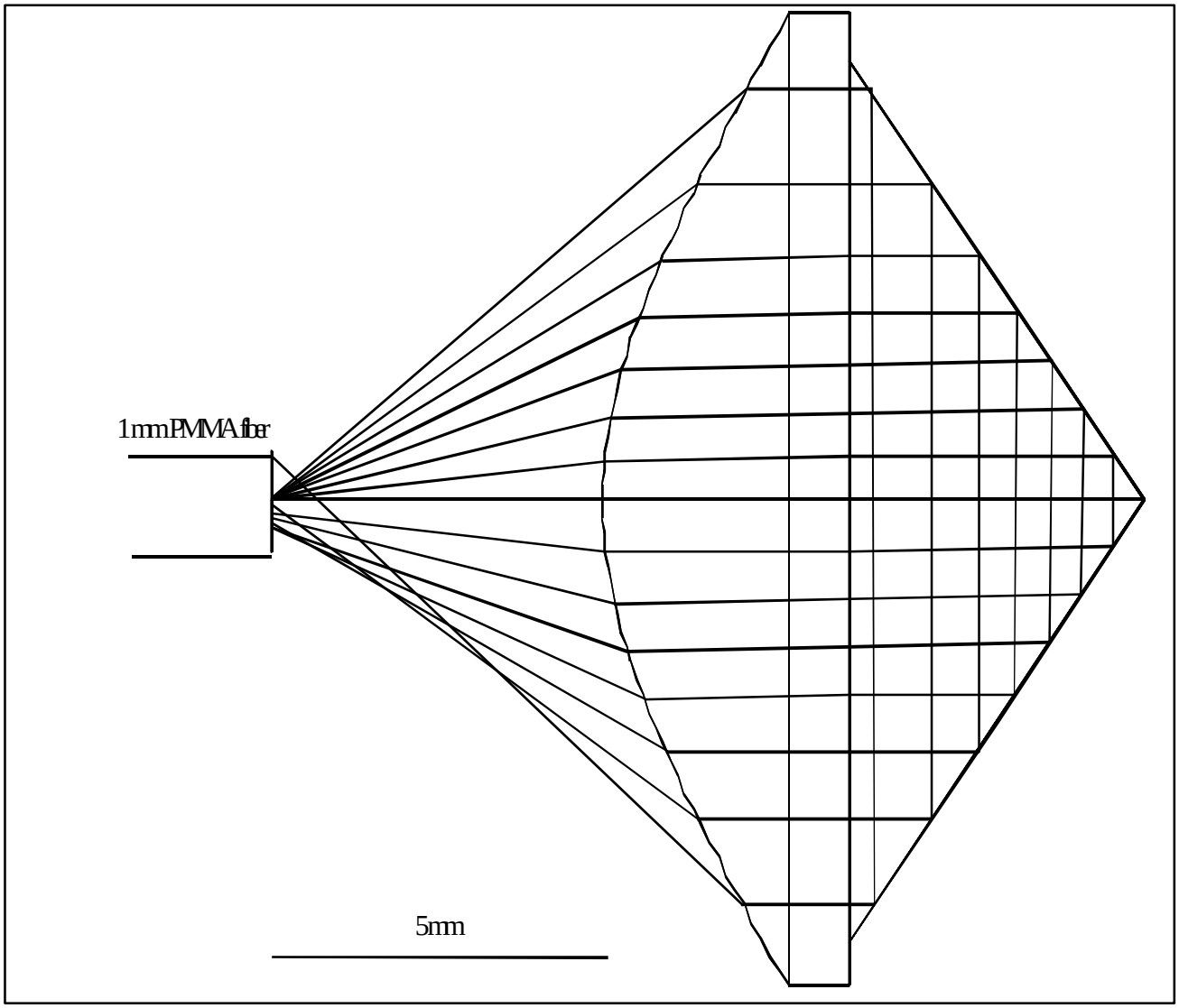

Figure 14. Design for a polymethylmethacrylate SPR optode. The lens portion is a conic section designed to minimize chromatic aberration and maximize signal return to the optical fiber.

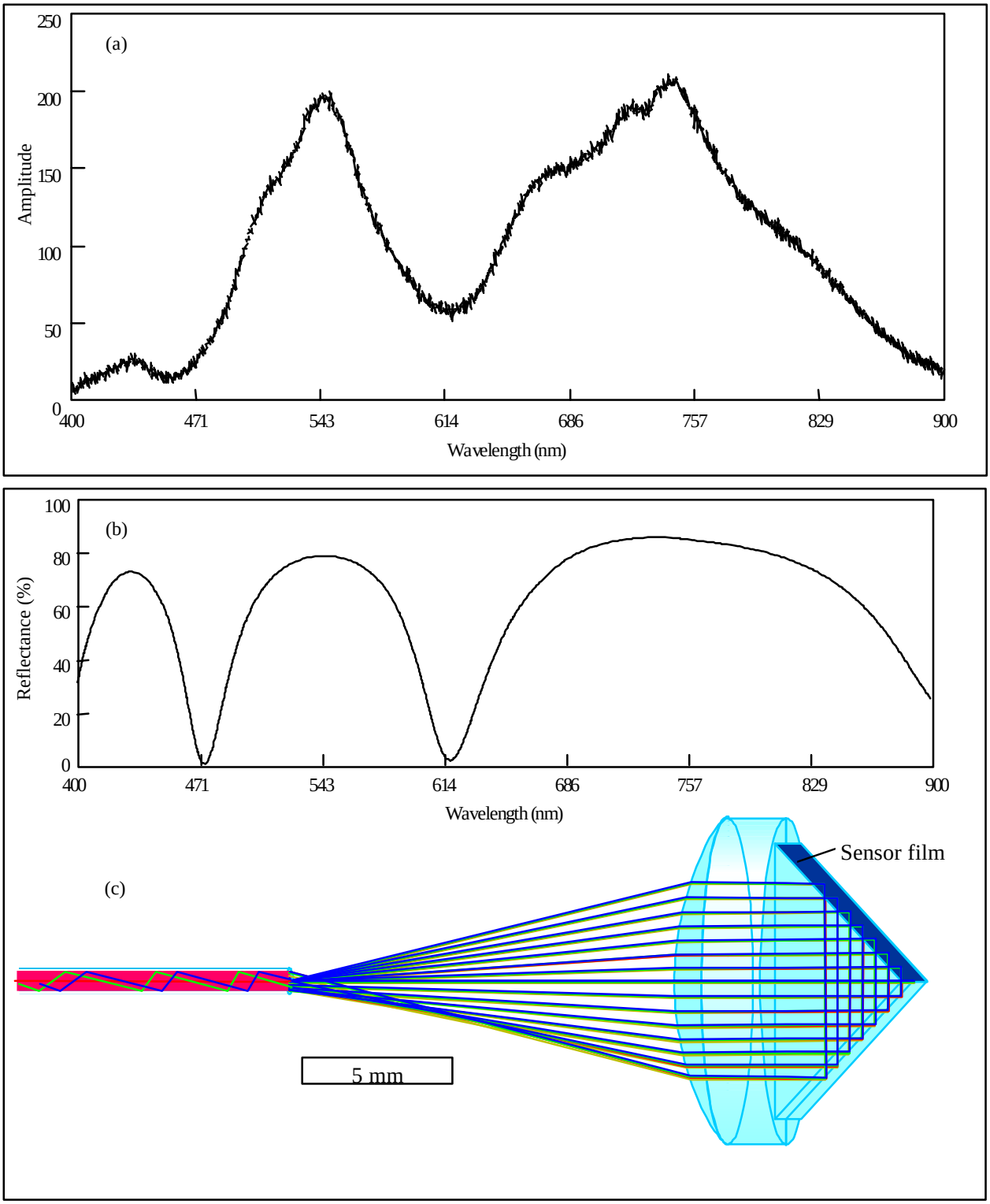

Figure 15. Design diagram of a glass optode made by cementing a plano-convex spherical lens to a 90° prism. The inset shows the SPR reflection spectrum (curve a) in comparison to the theoretically predicted reflectance (curve b).